

Helium Mass Flow Through a Solid-Superfluid-Solid Junction

Zhi Gang Cheng^{*} and John Beamish

Department of Physics, University of Alberta, Edmonton, Alberta, Canada T6G 2E1

Andrew D. Fefferman,[†] Fabien Souris,[‡] and Sébastien Balibar

Laboratoire de Physique Statistique de l'ENS, associé au CNRS et aux Universités Denis Diderot et Pierre et Marie Curie, 24 Rue Lhomond, 75231 Paris Cedex 05, France

Vincent Dauvois

DEN/DPC/SECR/LRMO, CEA Saclay, F-91191 Gif sur Yvette Cedex, France

(Received 6 February 2015; published 22 April 2015)

We report the results of flow experiments in which two chambers containing solid ^4He are connected by a superfluid Vycor channel. At low temperatures and pressures, mechanically squeezing the solid in one chamber produced a pressure increase in the second chamber, a measure of mass transport through our solid-superfluid-solid junction. This pressure response is very similar to the flow seen in recent experiments at the University of Massachusetts: it began around 600 mK, increased as the temperature was reduced, then decreased dramatically at a temperature, T_d , which depended on the ^3He impurity concentration. Our experiments indicate that the flow is limited by mass transfer across the solid-liquid interface near the Vycor ends, where the ^3He collects at low temperature, rather than by flow paths within the solid ^4He .

DOI: 10.1103/PhysRevLett.114.165301

PACS numbers: 67.80.bd, 62.20.-x, 67.80.bf

The quantum nature of solid ^4He gives it unique properties, the most dramatic possibility being super-solidity [1–3]. In 2004, torsional oscillator experiments [4,5] appeared to show the expected mass decoupling at low temperatures, but it is now clear [6–8] that the torsional oscillator anomalies originated in elastic changes [9,10] associated with dislocations. In solid ^4He , dislocations are extremely mobile and can reduce the solid's shear modulus by as much as 90%—an effect referred to as “giant plasticity” [10]. It has been proposed that some dislocations in ^4He have superfluid cores [11,12] which would allow new phenomena like “giant isochoric compressibility” [12], “superclimb” [13], and superflow in the dislocation network [11,14]. However, the most important open question involves mass flow. Early attempts to observe flow in solid ^4He were not successful. The first of these involved chambers connected by 200 μm diameter capillaries, with the entire system filled by solid ^4He at pressures in the range from 27 to 50 bar [15]. More recent experiments used a similar technique with chambers connected by an array of 25 μm glass capillaries [16]. Solid helium in one chamber (at around 36 bar) was compressed using a piezoelectrically driven diaphragm, and the pressure in the second chamber was measured to detect flow. Neither experiment showed flow at low temperatures. In the second experiment [16], thermally activated vacancy diffusion flow was observed near melting but decreased rapidly with temperature and was undetectable below 500 mK.

Recent experiments at the University of Massachusetts (UM) [17,18] have shown unexpected flow at low temperatures and generated considerable interest [19,20].

Chemical potential differences were applied across ^4He crystals, either by transmitting external pressure differences through Vycor “superfluid leads” [17] or by thermally generated fountain pressure gradients along the superfluid leads [18]. These experiments showed mass flow below 600 mK but only at pressures below about 28 bar. The magnitude of the flow rate was sample dependent but always increased as the temperature decreased then dropped suddenly at a temperature $T_d \approx 75$ mK (for samples with ^3He concentration $x_3 = 170$ ppb). This drop was associated with impurities [18]—increasing x_3 raised T_d and completely suppressed the mass flow below T_d . The flow above T_d was interpreted in terms of mass transport along dislocations whose cores might form a Luttinger liquid and the effect of impurities was attributed to ^3He binding to dislocations at low temperature and blocking flow paths.

Here, we report a new experiment also involving mass flow at low temperatures. The flow was generated in a cell, shown in Fig. 1, with a geometry that is essentially the inverse of the UM experiment. Instead of using two Vycor superfluid leads to apply a pressure difference across solid ^4He , we have two solid ^4He chambers connected by a superfluid-Vycor channel. One of the chambers (the “squeezing chamber”) has a flexible diaphragm which allows us to piezoelectrically compress the solid in it. The other “detecting chamber” contains a capacitive pressure gauge to detect flow of helium through the Vycor. Since pressure changes are mechanically transmitted through the solid helium to the Vycor ends, mass transport does not require flow through solid helium—pressure-driven

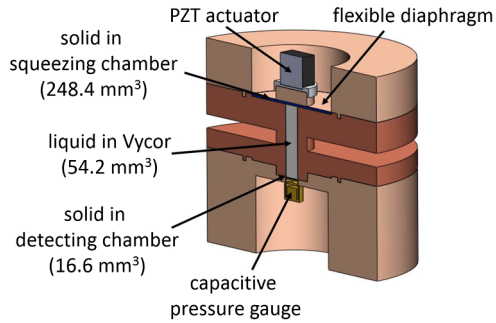


FIG. 1 (color online). The experimental cell. The bottom (“detecting chamber” side) was mounted on an experimental stage. A thin capillary (not shown) was connected to the detecting chamber.

transport across the solid-liquid interfaces is sufficient. This is closely related to UM “syringe” experiments [17], and intriguingly, our mass transfer has the same dependence on temperature, pressure, and ^3He concentration as the flow in the UM experiments [17,18].

Samples were prepared with the blocked-capillary method, as described in the Supplemental Material [21]. To look for flow, a dc voltage was applied to a piezoelectric actuator rigidly mounted against a 9.8 mm diameter “compression button” at the center of the diaphragm. This produced a uniform uniaxial compression of the solid helium over the surface of the 3.7 mm diameter Vycor rod. Beyond the edge of the button, the displacement was smaller and inhomogeneous. To calibrate the displacement, we used a liquid (25.2 bar) and a solid sample (26.9 bar). For the liquid, a low temperature compression of 150 V generated a 32 mbar pressure increase within a few seconds [21]. This cannot be used for calibration (since liquid leaves the cell during compression), but the rapid response guarantees that the Vycor is not a flow bottleneck when the ^4He is superfluid. For the solid sample, at high temperature (1.45 K) [21] where thermally activated vacancy diffusion ensures pressure equilibrium throughout the cell [16,22], the same 150 V squeeze generated a 100 mbar increase. This implies a 0.04% reduction of the cell volume, which corresponds to a displacement at the center of the diaphragm $\Delta d_s \approx 0.5 \mu\text{m}$ [21].

The thermally activated pressure response became slower and smaller as the temperature decreased, essentially disappearing by 700 mK. However, flow reappeared below about 600 mK with very different properties. Figure 2 shows the pressure changes in the detecting chamber for a typical 28.1 bar crystal grown from commercial ultrahigh purity (UHP) gas (which we analyzed to have $x_3 = 120 \text{ ppb} \pm 5\%$). After waiting for 10 minutes at each temperature, a 150 V squeeze was applied for 40 minutes and then removed. The total pressure change ΔP at each temperature is shown in Fig. 2(d). It was largest around 100 mK, gradually decreased at higher temperatures, and dropped rapidly below 80 mK, to less than half

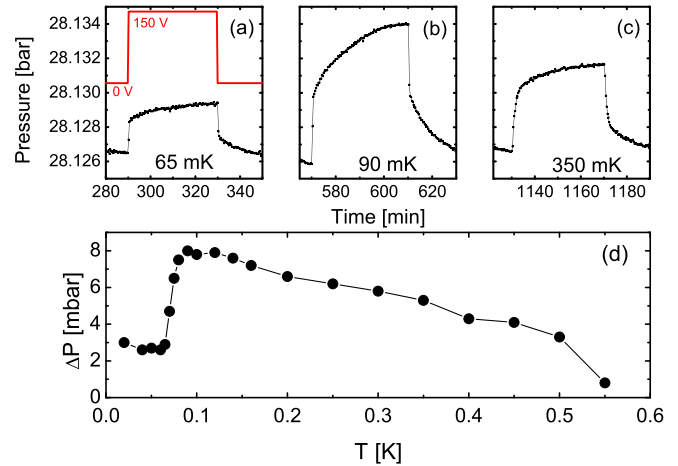


FIG. 2 (color online). (a),(b),(c) Pressure response for a 120 ppb sample at 65, 90, 350 mK, respectively. The red line in panel (a) indicates the voltage applied on the PZT (lead zirconium titanate) actuator. (d) Pressure response as a function of temperature.

the maximum value by 60 mK. This temperature dependence is strikingly similar to the flow rate measured in UM experiments. The pressure dependence is also similar; we consistently saw flow at pressures between 25 and 28 bar, but never above 28.2 bar.

The magnitude of the pressure change was sample dependent. The maximum value of ΔP varied from about 2 to 11 mbar in freshly grown samples, with no obvious dependence on pressure. It was reproducible if the sample was kept below 500 mK but often changed if thermally cycled beyond 600 mK. Note that ΔP is the pressure change during each 40 minute squeeze, rather than a flow rate $\partial P/\partial t$. We could determine flow rates from the slopes of pressure vs time curves but the shapes of the pressure response curves are temperature dependent, so selecting which slope to plot is somewhat arbitrary and produces large scatter. However, the general behavior is similar to that of ΔP as shown in Fig. 2(d) and to the UM flow results, although the average flow rates were much smaller in our experiments—about $2 \times 10^{-11} \text{ g/s}$, compared to $5 \times 10^{-8} \text{ g/s}$ in the UM measurements [18].

We also studied samples grown from gas with ^3He concentrations $x_3 = 20 \text{ ppm}$, 200 ppm, and 1 ppb. The 20 and 200 ppm samples were prepared by adding ^3He gas to the empty cell at 30 mK, then filling and pressurizing with UHP ^4He . The isotopically pure sample was prepared from gas with $x_3 = 1 \text{ ppb}$. The results are shown in Fig. 3 for crystals of the four isotopic purities, grown at similar pressures (27.7, 28.1, 26.9, and 26.6 bar for the 1 ppb, 120 ppb, 20 ppm, and 200 ppm samples, respectively). The general features are the same for all concentrations: flow begins around 600 mK, increases gradually as the temperature decreases, and suddenly drops and reaches a minimum at a temperature T_d (in the UM experiments, T_d was chosen where the flow started to drop). Adding ^3He raises

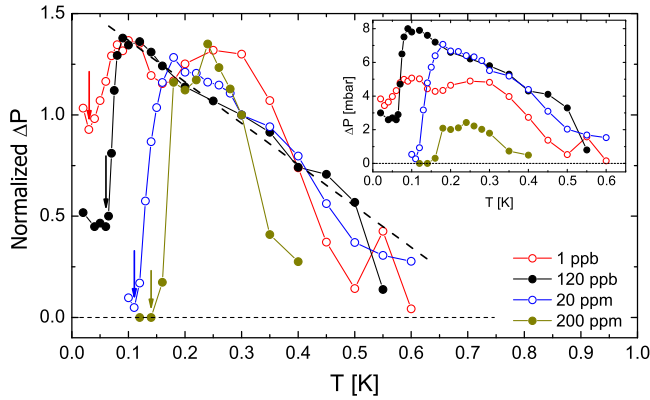


FIG. 3 (color online). Temperature dependence of normalized ΔP for samples with $x_3 = 1$ ppb, 120 ppb, 20 ppm, and 200 ppm. The data are normalized by ΔP at 0.3 K. The data for the 1 ppb sample, which was less stable, are multiplied by another factor of 1.3 in order to compare with the other samples. Inset: ΔP vs T for the same four samples.

T_d (to 110 mK for the 20 ppm and 140 mK for the 200 ppm sample) and the flow is suppressed more dramatically below T_d , completely disappearing for the 200 ppm ^3He sample. These features are essentially the same as for the flow rate in the UM experiments [18], but our measurements extend to lower temperatures and to much lower ^3He concentrations. The 1 ppb sample had the lowest T_d (around 30 mK) and the smallest reduction in flow below T_d (only about 25%).

The maximum pressure response below 600 mK is less than 11 mbar, much smaller than the pressure change at high temperature (100 mbar at $T = 1.45$ K), indicating that flow does not equilibrate the pressure in the entire squeezing chamber. At low temperatures, solid helium can sustain pressure gradients if the shear stresses are smaller than the critical stress for plastic flow, $\sigma_c \sim 40$ mbar [22]. This is the case for the compressions in our measurements [21], so only helium near the Vycor end is involved in the low temperature mass transfer; the solid further away can remain at the pressure generated by the initial compression. The fact that only part of the solid in the squeezing chamber contributes to the low temperature pressure response indicates that mass transport across the liquid-solid interface is due to the pressure directly transmitted to the Vycor surface by mechanical compression of the solid. This suggests that the bottleneck for the flow below T_d is at the Vycor surface, not along dislocations.

Since T_d depends on x_3 , we must consider the distribution of ^3He in our experiment. There are several regions in the cell with different impurity energies and low temperature ^3He concentrations. A ^3He atom dissolved in liquid ^4He at 25 bar has an energy 1.36 K lower than its energy in a perfect hcp ^4He crystal [28,29], so ^3He impurities will move from the solid to the liquid as the temperature is lowered. At 20 mK, even 0.1% liquid can remove essentially all ^3He from the solid ($x_{3S} < 10^{-20}$ for an average x_3

of 300 ppb [29]). In our cell, where about 17% of the helium is liquid in the Vycor pores, this effect is even more important. ^3He atoms are also attracted to dislocations, but the binding energy is only about 0.7 K [30] so the ^3He impurities will still move to the liquid at low temperatures. Vycor has a large internal pore surface, but because of the smaller zero-point energy of ^4He atoms, this silica surface is dominantly occupied by ^4He [31] and so does not affect x_3 significantly. The solid-liquid ($S-L$) interface is more important because it is known that ^3He atoms are strongly attracted to it, with a binding energy E_{SL} even larger than in liquid ^4He . However, measurements of E_{SL} are indirect, with values between -2 and -10 K inferred from experiments and calculations [32–35]. Since solid ^4He does not wet silica [36,37], the $S-L$ interfaces may extend beyond the pores and cover the Vycor ends. The interface area could be smaller than the geometric area of the Vycor ends (if the interface is confined to the pores) or larger (because the Vycor surfaces are rough).

We calculate the equilibrium ^3He concentrations using the fractions of atomic sites for each environment [21] and the relative energies for ^3He atoms, which we take as $E_S = 0$ K in solid ^4He , $E_{\text{dis}} = -0.7$ K on dislocations, and $E_L = -1.36$ K in the liquid in the Vycor. For the $S-L$ interface, we use the geometric area of the Vycor ends and an energy $E_{SL} = -2.5$ K, which gives behavior consistent with the x_3 dependence of T_d , as described below. Figure 4 shows the results for a typical dislocation density $\Lambda = 10^6/\text{cm}^2$. For an overall ^3He concentration of 120 ppb, the concentrations in the solid x_{3S} and on the dislocations $x_{3\text{dis}}$ both decrease as temperature is lowered. In the liquid, x_{3L} first increases and then becomes constant at low temperature, as expected. The only location where ^3He accumulates at low temperature is the $S-L$ interface.

Figure 4 also shows x_{3SL} for the other isotopic purity samples. For the 1 ppb ^3He sample, there is not enough ^3He in the cell to cover the $S-L$ interfaces and x_{3SL} saturates at a submonolayer coverage around 60 mK. For the other three samples, more than one ^3He layer can form at the interfaces. The ^3He coverage reaches one monolayer ($x_{3SL} = 1$) at higher temperature for higher x_3 : 80, 140, and 180 mK for the 120 ppb, 20 ppm, and 200 ppm samples, respectively. These temperatures are close to the T_d we observed. If we had chosen a larger (smaller) magnitude for E_{SL} , the values of T_d would have been higher (lower). There is evidence that ^3He trapped on dislocations is slow to unbind (>7 hours [38]) and to equilibrate with the liquid [39], but the $\sim 17\%$ of the ^3He initially in the liquid would still accumulate on the $S-L$ interfaces much more quickly. Without ^3He migrating from solid, the coverages and the temperatures at which a ^3He -rich layer forms would be lower, but ^3He would still form a layer with at least $\sim 17\%$ of the concentrations shown in Fig. 4. The ^3He coverage is also correlated with the reduction in flow below T_d . For the 1 ppb sample, there

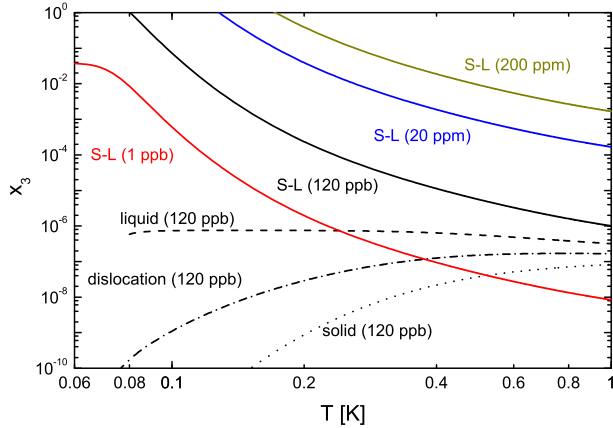


FIG. 4 (color online). Temperature dependence of ${}^3\text{He}$ concentrations at equilibrium. The solid lines are x_3 at the S - L interfaces for samples with different average concentrations. The dashed and dotted lines are x_3 at different environments in the 120 ppb sample.

is not enough ${}^3\text{He}$ to cover the S - L interfaces and the flow decreases only slightly. In the 120 ppb sample, there is enough for a few monolayers of ${}^3\text{He}$ and the flow is greatly reduced, but not eliminated. For higher ${}^3\text{He}$ concentrations, there is essentially no flow below T_d . This behavior strongly suggests that the bottleneck for flow is the S - L interfaces. Given the insolubility of ${}^4\text{He}$ atoms in liquid ${}^3\text{He}$, it seems plausible that a ${}^3\text{He}$ coverage of order one monolayer creates a barrier to mass transport of ${}^4\text{He}$ across the interfaces.

The fact that the equilibrium ${}^3\text{He}$ concentration on dislocations $x_{3\text{dis}}$ decreases at low temperatures argues against the drop at T_d being due to ${}^3\text{He}$ impurities blocking flow paths along dislocations. By 100 mK, $x_{3\text{dis}}$ is about 2×10^{-9} , far too low to pin dislocations or block flow along them (a single ${}^3\text{He}$ bound to a $100 \mu\text{m}$ long dislocation corresponds to $x_{3\text{dis}} = 3 \times 10^{-6}$). The concentration of ${}^3\text{He}$ may be larger near intersections of dislocations, where the binding is expected to be stronger. However, if ${}^3\text{He}$ remains trapped in the solid, even 1 ppb would be sufficient to completely saturate ($x_{3\text{dis}} = 1$) a typical dislocation network of density $10^6/\text{cm}^2$ (and much more than sufficient to saturate their intersections, which have far fewer binding sites [21]). We would then expect flow along dislocations to be completely blocked below T_d , rather than the small drop seen in the 1 ppb sample.

In contrast to our experiment, the UM superfluid-solid-superfluid sandwich does require flow through (or around) the solid, and their drop in flow at T_d was interpreted in terms of blocking dislocation flow paths. We suggest a different mechanism for the flow bottleneck, which should apply to the UM experiments since they also have a large liquid volume in the Vycor pores and solid-liquid interfaces at Vycor surfaces. Of course, our interpretation, of a flow bottleneck due to ${}^3\text{He}$ accumulating at the solid-liquid interface rather than on dislocations, does not explain

the nature of the flow between T_d and 600 mK, nor its temperature and pressure dependence. However, the behavior above T_d is remarkably similar in the two sets of measurements and it would be surprising if completely different physical mechanisms were involved.

In both experiments, the flow above T_d vanished at temperatures above 600 mK or pressures above 28 bar. This could indicate that a layer of superfluid ${}^4\text{He}$ at the S - L interface is required for flow. Since solid ${}^4\text{He}$ does not wet silica, at coexistence a liquid layer may cover the Vycor surface. The onset of flow at 600 mK could reflect a superfluid transition in such a film. Raising the pressure would reduce or eliminate the liquid layer at the interface [40], which could explain why low temperature flow is only observed below 28 bar.

In conclusion, we observed mass flow through a solid-superfluid-solid junction when pressure is applied by mechanically squeezing the solid ${}^4\text{He}$ at one end. This flow occurs when $T < 600$ mK, reaches a maximum at ~ 100 mK, and sharply decreases till a temperature T_d . T_d ranges from 30 to 140 mK when the average ${}^3\text{He}$ concentration is varied between 1 ppb and 200 ppm. Calculations of the ${}^3\text{He}$ distribution in our sample show that ${}^3\text{He}$ atoms accumulate at the solid-liquid interfaces as the temperature decreases, forming ${}^3\text{He}$ -rich layers at temperatures comparable to T_d . We suggest that the ${}^3\text{He}$ layers suppress the transfer of ${}^4\text{He}$ atoms across the interfaces, creating a bottleneck to flow.

We would like to thank Robert Hallock and Moses Chan for valuable discussions. This work was supported by a grant from NSERC Canada and by Grant No. ERC-AdG 247258 SUPERSOLID.

*czg0629@gmail.com

[†]Present address: Université Grenoble Alpes, Institut Néel, BP 166, 38042 Grenoble Cedex 9, France.

[‡]Present address: Department of Physics, University of Alberta, Edmonton, Alberta, Canada T6G 2E1.

- [1] A. F. Andreev and I. M. Lifshitz, *Sov. Phys. JETP* **29**, 1107 (1969).
- [2] A. J. Leggett, *Phys. Rev. Lett.* **25**, 1543 (1970).
- [3] G. Chester, *Phys. Rev. A* **2**, 256 (1970).
- [4] E. Kim and M. H. W. Chan, *Science* **305**, 1941 (2004).
- [5] E. Kim and M. H. W. Chan, *Nature (London)* **427**, 225 (2004).
- [6] J. R. Beamish, A. D. Fefferman, A. Haziot, X. Rojas, and S. Balibar, *Phys. Rev. B* **85**, 180501 (2012).
- [7] H. J. Maris, *Phys. Rev. B* **86**, 020502 (2012).
- [8] D. Y. Kim and M. H. W. Chan, *Phys. Rev. Lett.* **109**, 155301 (2012).
- [9] J. Day and J. R. Beamish, *Nature (London)* **450**, 853 (2007).
- [10] A. Haziot, X. Rojas, A. D. Fefferman, J. R. Beamish, and S. Balibar, *Phys. Rev. Lett.* **110**, 035301 (2013).

- [11] M. Boninsegni, A. B. Kuklov, L. Pollet, N. V. Prokof'ev, B. V. Svistunov, and M. Troyer, *Phys. Rev. Lett.* **99**, 035301 (2007).
- [12] S. G. Soyler, A. B. Kuklov, L. Pollet, N. V. Prokof'ev, and B. V. Svistunov, *Phys. Rev. Lett.* **103**, 175301 (2009).
- [13] D. Aleinikava, E. Dedits, and A. Kuklov, *J. Low Temp. Phys.* **162**, 464 (2011).
- [14] S. Shevchenko, *Sov. J. Low Temp. Phys.* **13**, 61 (1987).
- [15] D. S. Greywall, *Phys. Rev. B* **16**, 1291 (1977).
- [16] J. Day and J. Beamish, *Phys. Rev. Lett.* **96**, 105304 (2006).
- [17] M. W. Ray and R. B. Hallock, *Phys. Rev. Lett.* **100**, 235301 (2008); *Phys. Rev. B* **79**, 224302 (2009); *J. Low Temp. Phys.* **162**, 427 (2011).
- [18] M. W. Ray and R. B. Hallock, *Phys. Rev. Lett.* **105**, 145301 (2010); *Phys. Rev. B* **82**, 012502 (2010); **84**, 144512 (2011); Y. Vekhov and R. B. Hallock, *Phys. Rev. Lett.* **109**, 045303 (2012); Y. Vekhov, W. J. Mullin, and R. B. Hallock, *Phys. Rev. Lett.* **113**, 035302 (2014); Y. Vekhov and R. B. Hallock, *Phys. Rev. B* **90**, 134511 (2014).
- [19] A. B. Kuklov, L. Pollet, N. V. Prokof'ev, and B. V. Svistunov, *Phys. Rev. B* **90**, 184508 (2014).
- [20] R. B. Hallock, *J. Low Temp. Phys.* (2015).
- [21] See Supplemental Material at <http://link.aps.org/supplemental/10.1103/PhysRevLett.114.165301>, which includes [22–27], for technical details of experimental cell, sample preparation, calibration of diaphragm displacement, pressure gradient within sample, and calculations of ^3He distribution.
- [22] A. Suhel and J. R. Beamish, *Phys. Rev. B* **84**, 094512 (2011).
- [23] [http://www.piceramic.com/ Model 141-03](http://www.piceramic.com/Model%20141-03).
- [24] J. Beamish, *J. Low Temp. Phys.* **168**, 194 (2012).
- [25] C. Boghosian and H. Meyer, *Phys. Rev.* **152**, 200 (1966); **163**, 206 (1967).
- [26] P. Debye and R. L. Cleland, *J. Appl. Phys.* **30**, 843 (1959).
- [27] E. Molz and J. Beamish, *J. Low Temp. Phys.* **101**, 1055 (1995).
- [28] D. O. Edwards and S. Balibar, *Phys. Rev. B* **39**, 4083 (1989).
- [29] X. Rojas, C. Pantalei, H. Maris, and S. Balibar, *J. Low Temp. Phys.* **158**, 478 (2010).
- [30] F. Souris, A. D. Fefferman, H. J. Maris, V. Dauvois, P. Jean-Baptiste, J. R. Beamish, and S. Balibar, *Phys. Rev. B* **90**, 180103 (2014).
- [31] N. Mulders, J. Ma, S. Kim, J. Yoon, and M. Chan, *J. Low Temp. Phys.* **101**, 95 (1995).
- [32] E. Rolley, S. Balibar, C. Guthmann, and P. Nozières, *Physica (Amsterdam)* **210B**, 397 (1995).
- [33] J. Treiner, *J. Low Temp. Phys.* **92**, 1 (1993).
- [34] A. Y. Parshin, *J. Low Temp. Phys.* **110**, 133 (1998).
- [35] C.-L. Wang and G. Agnolet, *J. Low Temp. Phys.* **89**, 759 (1992).
- [36] S. Sasaki, F. Caupin, and S. Balibar, *J. Low Temp. Phys.* **153**, 43 (2008).
- [37] S. Balibar, *C. R. Physique* **14**, 531 (2013).
- [38] X. Rojas, A. Haziot, and S. Balibar, *J. Phys. Conf. Ser.* **400**, 012062 (2012).
- [39] X. Rojas, A. Haziot, V. Bapst, S. Balibar, and H. J. Maris, *Phys. Rev. Lett.* **105**, 145302 (2010).
- [40] J. G. Dash and J. S. Wettlaufer, *Phys. Rev. Lett.* **94**, 235301 (2005).